AD-A252 874

(2)

OFFICE OF NAVAL RESEARCH

Grant N00014-91-J-1550

R&T Code: 413w003

Technical Report No. 10

Chemistry of hydrogen on diamond (100)

by

Y. L. Yang, L. M. Ulvick, L. F. Sutcu, and M. P. D'Evelyn

DTIC
ELECTE
JUL 16 1992
S A D

Prepared for publication in

Thin Solid Films

Rice University
Department of Chemistry
Houston, TX 77251-1892

92-18884

June 29, 1992

Reproduction, in whole or in part, is permitted for any purpose of the United States Government.

This document has been approved for public release and sale; its distribution is unlimited.

92 7 15 074

REPORT DOCUMENTATION PAGE

Form Approved
OMB No. 0704-0188

Public reporting burden for this collection of information is estimated to average 1 hour per response, including the time for reviewing instructions, searching existing data sources, gathering and maintaining the data needed, and completing and reviewing the collection of information. Send comments regarding this burden estimate or any other aspect of this collection of information, including suggestions for reducing this burden, to Washington Headquarters Services, Directorate for information Operations and Reports, 1215 Jefferson Davis Highway, Suite 1204, Arlington, VA 22202-4302, and to the Office of Management and Budget, Paperwork Reduction Project (0704-0188), Washington, DC 20503.

1. AGENCY USE ONLY (Leave blank)	2. REPORT DATE	3. REPORT TYPE AND DATES COVERED
	June 1992	Technical

4. TITLE AND SUBTITLE
Chemistry of hydrogen on diamond (100)

5. FUNDING NUMBERS
Grant #:
N00014-91-J-1550

6. AUTHOR(S)
Y. L. Yang, L. M. Ulvick, L. F. Sutcu,
and M. P. D'Evelyn

7. PERFORMING ORGANIZATION NAME(S) AND ADDRESS(ES)
Rice University
Department of Chemistry
Houston, TX 77251-1892

8. PERFORMING ORGANIZATION REPORT NUMBER
Technical Report
#10

9. SPONSORING/MONITORING AGENCY NAME(S) AND ADDRESS(ES)
Office of Naval Research
800 N. Quincy Street
Arlington, VA 22217-5000

10. SPONSORING/MONITORING AGENCY REPORT NUMBER

11. SUPPLEMENTARY NOTES
Prepared for publication in:
Thin Solid Films.

12a. DISTRIBUTION/AVAILABILITY STATEMENT
Approved for public release; distribution is unlimited.

12b. DISTRIBUTION CODE

13. ABSTRACT *(Maximum 200 words)*

Hydrogen plays a crucial role in diamond film growth by chemical vapor deposition and is likely to be similarly critical to atomic layer epitaxy, yet the surface chemistry of hydrogen on diamond is only beginning to be understood. We have investigated the adsorption of hydrogen and deuterium on diamond (100) by temperature-programmed desorption and by infrared multiple-internal-reflection spectroscopy using a natural type IIa diamond internal reflection element. Complementary theoretical studies have been carried out using the empirical MM3 molecular mechanics force field, which has a demonstrated high degree of accuracy for many molecules despite computational simplicity. H_2 desorption was observed with a peak temperature of ≈1250 K and a peak shape suggestive of first-order kinetics. Assuming a preexponential factor of 10^{13} sec^{-1}, the activation energy for desorption is estimated as ≈80 kcal/mol. Infrared evidence was seen for the monohydride surface structure, with one hydrogen atom per surface carbon atom (δ_{CD} mode at 901 cm^{-1}). The MM3 calculations predict that the (2×1):H monohydride phase is the most stable thermodynamically and the dominant phase under typical chemical vapor deposition conditions.

14. SUBJECT TERMS
Diamond, hydrogen, desorption kinetics, infrared spectroscopy, molecular mechanics

15. NUMBER OF PAGES

16. PRICE CODE

17. SECURITY CLASSIFICATION OF REPORT	18. SECURITY CLASSIFICATION OF THIS PAGE	19. SECURITY CLASSIFICATION OF ABSTRACT	20. LIMITATION OF ABSTRACT
Unclassified	Unclassified	Unclassified	

Chemistry of hydrogen on diamond (100)

Yuemei L. Yang, Lisa M. Ulvick, Leyla F. Sutcu, and Mark P. D'Evelyn

Department of Chemistry and Rice Quantum Institute, Rice University, Houston, TX 77251-1892

Abstract

Hydrogen plays a crucial role in diamond film growth by chemical vapor deposition and is likely to be similarly critical to atomic layer epitaxy, yet the surface chemistry of hydrogen on diamond is only beginning to be understood. We have investigated the adsorption of hydrogen and deuterium on diamond (100) by temperature-programmed desorption and by infrared multiple-internal-reflection spectroscopy using a natural type IIa diamond internal reflection element. Complementary theoretical studies have been carried out using the empirical MM3 molecular mechanics force field, which has a demonstrated high degree of accuracy for many molecules despite computational simplicity. H_2 desorption was observed with a peak temperature of ≈1250 K and a peak shape suggestive of first-order kinetics. Assuming a preexponential factor of 10^{13} sec^{-1}, the activation energy for desorption is estimated as ≈80 kcal/mol. Infrared evidence was seen for the monohydride surface structure, with one hydrogen atom per surface carbon atom (δ_{CD} mode at 901 cm^{-1}). The MM3 calculations predict that the (2×1):H monohydride phase is the most stable thermodynamically and the dominant phase under typical chemical vapor deposition conditions.

Paper P-2 presented at the *Second International Symposium on Atomic Layer Epitaxy*

Submitted to *Thin Solid Films*

Dist | Avail and/or Special

A-1

I. INTRODUCTION

The critical role played by hydrogen in diamond chemical vapor deposition (CVD) is well established [1]. To date only preliminary results have been published on the growth of diamond films by atomic layer epitaxy (ALE) [2], but surface hydrogen plays a crucial role in ALE growth of silicon [3,4], and will certainly be important in diamond ALE processes currently being developed. Despite its obvious importance, the surface chemistry of hydrogen on diamond is only beginning to be understood. Of the two crystal faces which are prevalent in CVD-grown diamond films, the properties of the clean and hydrogenated (111) face are much better understood than those of the (100) face. However, the (100) face is the only low-index orientation where the actual surface of CVD films resembles the nominal orientation (i.e., the surface is smooth on the nanometer-to-micron scale) [5], and is the orientation most likely to be useful for atomic layer epitaxy. Nominally clean diamond (100) has been observed to have a (2×1) unit cell by low energy electron diffraction [6]. By analogy to the well-studied Si(100) and Ge(100) surfaces, the (2×1) unit cell suggests the formation of dimer bonds between pairs of surface carbon atoms, as illustrated schematically in Fig. 1(a). Hydrogen atoms are known to chemisorb on diamond (100) [7-10], with either a (2×1) [8,9] or nominally (1×1) [8] unit cell. The most transparent assignments for these structures, by analogy to the better-studied H/Si(100) system, are a (2×1):H monohydride, with one hydrogen atom per surface carbon atom (Fig. 1(b)) and a (1×1):2H dihydride, with two hydrogen atoms per surface carbon atom (Fig. 1(c)), respectively.

Hamza *et al.* [8] reported temperature-programmed desorption (TPD) results for hydrogen on diamond (100), with the peak desorption rate occurring at a substrate temperature near 1200 K at low initial coverage. Based on their observation, by electron-stimulated desorption, of the continued presence of surface hydrogen even after annealing to 1400 K and their inability to detect unoccupied surface states, Hamza *et al.* assigned the TPD peak to hydrogen in the (1×1):2H dihydride state (Fig. 1(c)) desorbing, leaving hydrogen in the (2×1):H monohydride state (Fig. 1(b)). Several aspects of this assignment are troubling, however. First, the structural similarity of diamond and silicon surfaces suggests that the behavior of hydrogen on the two materials will be qualitatively similar even if the energetics are different. H_2 desorbs from the monohydride state on both Si(100) and Si(111) near 800 K, yielding the clean surface, although the details of the desorption kinetics are different on the two crystal faces [11]. On diamond (111), the monohydride, with a (1×1) near-ideal bulk-terminated structure [12], desorbs upon heating to ≈1200 K, yielding a clean surface with a (2×1) unit cell [13-15]. The similarities in the desorption temperatures of H_2 on diamond (100) and (111) and the analogy to silicon suggests, therefore, that the observed desorption on diamond (100) near 1200 K is taking place from the *monohydride* rather than from the dihydride. A second difficulty with the desorption assignment is that steric repulsion between hydrogen atoms in the (1×1):2H dihydride should be extreme. The corresponding monohydride and dihydride species on Si(100) have a substantial literature and it appears that a full dihydride can only be formed under

conditions where SiH_3(a) is also formed and some etching takes place, and that steric repulsion between the hydrogen atoms is important [16]. The lattice constant of diamond is 34% smaller than that of silicon and hydrogen-hydrogen repulsion will be even more important. If the hydrogen atoms on diamond (1×1):2H remained in their ideal sp^3 positions, the distance between neighboring (nonbonded) hydrogen atoms would be only 0.71 Å, less than the H-H bond length in H_2! If this structure exists, therefore, one should expect rather dramatic orientational changes in the C-H bonds in order to stabilize the surface. Such changes will cost energy, perhaps enough to make the (1×1):2H dihydride thermodynamically unstable with respect to dehydrogenation to the monohydride. Indeed, our calculations [17], along with recent semiempirical calculations [18], predict that the (1×1):2H full dihydride is unstable, although the quantitative reliability of the calculations is uncertain. A final difficulty with the assignment by Hamza *et al.* [8] is that a subsequent experiment by Thomas *et al.* [9] also observed a hydrogen desorption peak near 1220 K, but observed (2×1) diffraction patterns both before and after desorption. The latter observation can be explained by a substantial activation barrier for H-atom attack on the C-C dimer bond in the monohydride (Fig. 1(b)) [9b], and suggests, in accord with the argument presented above, that the desorption peak is due primarily to hydrogen atoms in the monohydride structure and that the diamond surface is essentially clean following desorption.

Although we believe that the (1×1):2H full dihydride is not important in diamond CVD under typical growth conditions, dihydride (CH_2) structures with hydrogen coverages less than two full monolayers *are* likely to be important. For example, a (3×1) structure may be generated by inserting a monohydride dimer between dihydride units at a hydrogen coverage of 1.33 monolayer. The analogous (3×1):1.33H structure on Si(100) is well established [16], and steric repulsion is nearly eliminated.

We have investigated the interaction of hydrogen with diamond (100) by TPD, by infrared spectroscopy, and by theoretical molecular mechanics calculations. Infrared spectroscopy should readily be able to distinguish between different forms of surface hydrogen, and we believe that molecular mechanics is very useful for predicting the structure and energetics of surface species on covalent solids such as diamond.

II. EXPERIMENTAL

The temperature-programmed desorption (TPD) and infrared spectroscopic experiments were performed in the ultrahigh vacuum chamber shown schematically in Fig. 2. The analysis chamber is pumped via a liquid-N_2-trapped diffusion pump and titanium sublimation pump (base pressure ≈ 1 - 2 × 10^{-10} Torr), and is equipped with a quadrupole mass spectrometer (UTI 400C), a cylindrical mirror analyzer for Auger electron spectroscopy, homebuilt LEED/ESDIAD optics, and a tungsten filament used for atomic H dosing [19,20].

Separate diamond (100) samples were used in the TPD and infrared experiments. Type Ia diamond (100) samples, $6.5 \times 3.5 \times 0.5$ mm^3 in dimension (DRI, Inc.), were used in the TPD experiments. The samples were obtained in as-sawn condition and were polished on a high-speed iron scaife with diamond powder in olive oil [20]. Our initial TPD experiments utilized a Ta foil holder/heater for the diamond, but this proved to be unsatisfactory as atomic hydrogen dissolves readily in bulk Ta [21]. We found that TPD spectra taken without the diamond in the holder were indistinguishable from data taken with the diamond, implying that most of the desorbing hydrogen originated from the bulk of the Ta foil [22]. A second difficulty with the foil sample holder scheme is that accurate sample temperatures are difficult to obtain. Unlike silicon, diamond does not glow at temperatures near 1000 K and so optical pyrometry cannot be used to provide a temperature correction.

The TPD results presented below were obtained using a modified sample holder scheme, which has significant advantages in terms of reduced outgassing and capability for accurate sample temperature calibration. A W film, 0.5 μm thick, was sputter-deposited on the back of the diamond (100) sample. Hydrogen desorbs from W below 600 K [23], and therefore should not interfere with the desorption signal due to the diamond. The sample was held at each end between two sets of W wire clips, 0.254 mm in diameter, which in turn were electrically isolated and attached to a cooled Cu block. A pair of chromel-alumel thermocouples were placed in direct contact with the sample underneath one of the wire clips. The sample was heated by passing current between the pair of clips through the W film on the back. As the thermal contact between the W film and the sample should be excellent, the temperature of the W should accurately reflect that of the diamond, even if the thermocouple-derived temperature is in error. We performed careful temperature calibrations by optical pyrometry of the W film through the diamond. As the emissivity of the W/diamond interface was not known, we prepared a second diamond sample with a W film on the back and placed it in a tubular furnace within the UHV analysis chamber. We used the second sample, whose temperature should be equal to that of the furnace (measured with a chromel-alumel thermocouple), to calibrate the pyrometer [20]. Near temperatures of 973 K, the thermocouple pressed against the sample was found to be accurate to within 10-20 K, but the temperature error rose to 140 K (with the thermocouple reading too low) at a sample temperature of 1473 K. We estimate that the calibrated temperatures are correct to within $\approx \pm 25$ K.

Temperature ramps for TPD were generated using a standard DC power supply controlled by a commercial PID temperature controller (Eurotherm 818P) interfaced to an IBM-AT-compatible personal computer. The output of the mass spectrometer was digitized by a data acquisition board in the same computer, allowing acquisition of temperature-programmed desorption or residual gas analysis data [20]. A heating rate of 5 K s^{-1} was used in the TPD experiments reported here.

Diamond cannot be sputtered and annealed without extensive graphitization [6,24], but several groups have shown that heating a freshly polished diamond sample in UHV to $\approx$ 1300 K desorbs

oxygen and generates a clean (except possibly for hydrogen) diamond surface [6,8,13,25,26]. We have followed this procedure. Atomic hydrogen exposures were performed by backfilling the UHV analysis chamber with H_2 to pressures of 5×10^{-7}–5×10^{-5} Torr and heating a coiled W filament located ≈ 2 cm from the sample to 1700-1800 K. Because of the difficulty in calibrating accurate atomic hydrogen exposures made in this way, we simply report the apparent exposures to molecular hydrogen as Langmuirs (1 L ≡ 10^{-6} Torr sec), without an ion gauge correction.

We have performed preliminary infrared multiple-internal reflection spectroscopy (IMIRS) [27,28] experiments in the reactor cell shown in Fig. 2(b). IMIRS is a high-sensitivity technique for obtaining high-resolution vibrational spectra of sub-monolayer quantities of adsorbates on substrates which are transparent in the infrared. IMIRS takes advantage of the phenomenon of total internal reflection to gain sensitivity to surface vibrational modes by using many internal reflections. We have a type IIa natural diamond internal reflection element (IRE), $15 \times 3 \times 0.22$ mm^3 in dimension, with a (100) orientation on the large-area faces. The end faces of the IRE are beveled at 45°, providing ≈33 internal reflections from each long face, as illustrated schematically in Fig. 2(c). The optical coupling scheme is shown in Fig. 2(b). Collimated light from a Fourier-transform infrared spectrometer (Mattson Cygnus 100) is focused by an off-axis paraboloidal mirror through a differentially-pumped KBr window onto one bevelled edge of the diamond IRE. Light transmitted through the opposite end of the IRE is collected and focused onto a detector (narrow-band HgCdTe, Graseby Infrared) by two additional off-axis paraboloidal mirrors.

Exposures of the diamond (100) IRE to atomic hydrogen or deuterium were made by backfilling the reactor cell with H_2 or D_2, respectively, at pressures between 1×10^{-7} and 2×10^{-6} Torr for up to two hours, and heating a W filament located ≈ 1 cm from the sample to 1700-1800 K.

III. MOLECULAR MECHANICS CALCULATIONS

The calculation method used to calculate the structures and enthalpies of formation of clean and hydrogenated diamond (100) has been described in detail previously [17]. The third-generation MM3 force field, with parameters for saturated, unsaturated, and conjugated hydrocarbons, has a demonstrated high degree of accuracy (bond lengths ≈ ±0.01 Å, bond angles between atoms other than hydrogen ≈ ±1°, torsional angles ≈ ±4°, heats of formation ≈ ±1 kcal/mol) for small, large, and highly strained molecules and bulk diamond as well [29,30]. MM3 should be applicable to the description of saturated, unsaturated, and conjugated hydrocarbon species on any crystal face of diamond as long as the bond lengths, bond angles, and distances between nonbonded atoms are within the range of values in structures for which MM3 has demonstrated accuracy. MM3 parameters for radicals are tentative [30,31], making calculations with open-shell species more uncertain, and MM3 cannot describe surface species with bonding configurations that have not been parameterized in molecules.

Atomic positions were determined by minimizing an empirical potential energy function, the so-called steric energy E [29,30], subject to periodic boundary conditions and a substrate lattice constant fixed at the value of bulk diamond [17]. Enthalpies of formation were calculated by adding bond enthalpies (ΔH_{bond}) and functional-group correction terms (ΔH_{struct}) to the minimized steric energy for various surface species.

IV. RESULTS AND DISCUSSION

TPD results for H_2 desorbing from diamond (100) are shown in Fig. 3. The peak desorption rate occurs at $T_p \approx 1250$ K, and the peak has the asymmetric shape characteristic of first-order desorption. Better evidence for first-order desorption may be derived from an independence of T_p on the initial surface coverage [32,33]. However, we have not yet been able to establish the dependence of T_p on coverage due to poor signal-to-noise ratio. The peak temperature (1250 K) agrees well with those of Hamza *et al.* [8], 1200 K at low coverage, and of Thomas *et al.* [9], ≈1220 K. Assuming a preexponential factor of 10^{13} sec^{-1}, the activation energy for desorption may be estimated as ≈ 79.5 kcal/mol [32]. A calculated TPD spectrum, assuming first-order desorption, a preexponential factor of 10^{13} sec^{-1}, and an activation energy of 79.5 kcal/mol is also plotted in Fig. 3. The semiquantitative agreement in the measured and calculated peak shapes supports our assignment of first-order desorption and the approximate value of the preexponential factor. The "normal" value of the preexponential factor for hydrogen desorption indicated by our data contrasts with the results of Hamza *et al.* [8] and of Thomas *et al.* [9] on diamond (100) and of Schulberg *et al.* [34] on polycrystalline CVD-grown diamond films. Each of these authors obtained significantly broader TPD peaks than that shown in Fig. 3, implying apparent preexponential factors in the range of 3×10^5 to 5×10^7 sec^{-1} [34]. Differences in sample preparation may be responsible for the disparate results, as desorption from steps and defect sites might occur at slightly different rates and might give rise to anomalously broad TPD peaks.

Another intriguing feature of the TPD spectrum is an apparent shoulder near 1125 K, ≈75 K below T_p. The limited signal-to-noise ratio makes it impossible to determine if this is a true shoulder, but it is well established that desorption from dihydride species on silicon (SiH_2 groups) gives rise to a secondary TPD peak about 100 K lower in temperature than the monohydride (SiH) peak near 800 K [16e,35]. On Ge(100), hydrogen adsorption at above one monolayer coverage (implying dihydride formation) gives rise to a shoulder about 40 K below the monohydride peak desorption temperature at 570 K [36]. If the shoulder in Fig. 3 is real, it may indicate desorption from dihydride species, by analogy to the behavior of hydrogen on Si and Ge.

The poor signal-to-noise ratio in Fig. 3 is due to background hydrogen desorption from supports, despite the fact that hot surface areas on the sample holder were kept to a bare minimum. The rising background became quite significant above 1200 K. The background can be partially compensated for by taking the difference between TPD spectra obtained and before H dosing, and

this was done with the data shown in Fig. 3. However, imperfect cancellation is responsible for the sharp rise in the background above 1300 K. A satisfactory solution to the background desorption problem should be achievable by adding differential pumping to the mass spectrometer.

The results of MM3 calculations of the structures of the surface species illustrated in Fig. 1 are summarized in Fig. 5 [17]. The structures are entirely consistent with the qualitative conclusions which might be drawn from simple bond length and van der Waals radius considerations. The dimerized surface atoms on the (2×1) clean surface (Figs. 1(a), 5(a)) are linked by highly pyramidalized double bonds, where the normal C=C bond length of 1.34 Å is calculated to increase to 1.46 Å, and the dihedral angle between the dimer bond and the back bonds to the second-layer atoms is nearly 60°, far from the ideal sp^2 planar geometry. The strain due to the backbonds also increases the C-C single bond length in the (2×1):H monohydride structure (Figs. 1(b), 5(b)) from its unstrained value of 1.54 Å to 1.63 Å. Finally, the extreme steric repulsion between neighboring, non-bonded hydrogen atoms in the (1×1):2H full dihydride structure (Figs. 1(c), 5(c)) causes a reduction in the H-C-H angle and twisting by some 26° about the surface normal. The extreme steric repulsion of the (1×1):2H full dihydride is eliminated in the (3×1):1.33H structure(Fig. 5(d)).

The energetic predictions of the MM3 calculations can be summarized the by following enthalpies of reaction at 298 K, expressed with respect to the (2×1):H monohydride:

$$\text{C(100)-(2×1):H} \rightarrow \text{C(100)-(2×1)} + \text{H}_2 \qquad \Delta H^\circ_{298} = +46.7 \text{ kcal/mol} \quad (1)$$

$$\text{C(100)-(2×1):H} + \text{H}_2 \rightarrow 2\ \text{C(100)-(1×1):2H} \qquad \Delta H^\circ_{298} = +49.2 \text{ kcal/mol} \quad (2)$$

$$3\ \text{C(100)-(2×1):H} + \text{H}_2 \rightarrow 2\ \text{C(100)-(3×1):1.33H} \qquad \Delta H^\circ_{298} = -15.6 \text{ kcal/mol} \quad (3)$$

The implication of the positive heat of reaction for Eq. (2) is that we predict the the (1×1):2H full dihydride is indeed thermodynamically unstable, as the system may reduce its energy by 49 kcal/mol by desorption of H_2, producing the monohydride.

We find MM3 to be a computationally convenient yet very powerful tool for calculating the structure and energetics of surface species on diamond. The method makes the clear prediction that the monohydride is the most stable species and the one which is likely to predominate under typical CVD conditions. However, because the amount of strain and steric repulsion which is present in the (2×1) clean and (1×1):2H structures on diamond (100) considerably exceeds that in any molecules for which the (empirical) MM3 method has been demonstrated to be quantitatively accurate, comparisons of our results to predictions of high level quantum chemical calculations are needed.

An IMIRS spectrum of diamond (100) following an exposure to atomic deuterium at a sample temperature of ≈ 500 K is shown in Fig. 4. A peak observed at a frequency of 901 cm^{-1} is assigned to a C-D deformation mode. This assignment is based on the similarity of the frequency of the surface vibrational mode to CC-D bending modes of 901 and 918 cm^{-1} in adamantane-d_{16} [37] and $(CD_3)_3C$-D [38], respectively. The peak has a full width at half maximum of ≈ 20 cm^{-1}, comparable

to that seen for the C-H stretching mode on diamond (111) [39] and the Si-H stretching mode on flat Si(100) [27(c)]. The linewidth for H on flat Si(100) was overwhelmingly due to inhomogeneous broadening [27(c)], which is almost certainly also the source of the linewidth seen here. The diamond (100) internal reflection element sample was "as-polished" when inserted in the chamber, with a standard roughness quoted by the vendor as 40 nm. We recently observed, by atomic force microscopy, that an as-polished diamond (111) sample had a high density of ridges and scratches from the polishing, with most of the features 5-10 nm in height [5b]. If, as seems likely, similar features were present on our (100)-oriented IRE, they likely would not have been removed by a mild anneal and could easily account for the infrared linewidth. Several other infrared peaks have been observed, including features that may be associated with CH species. However, we have found that trace amounts of hydrocarbon impurities are present in the infrared detector and that miscancellation between background and sample scans can lead to spurious CH peaks, and we have not yet been able to unambiguously distinguish the surface peaks from the detector (spurious) peaks.

Our preliminary IMIRS results show evidence for the monohydride, whose bending frequency has been observed here for the first time. The closeness of the peak frequency (901 cm^{-1}) to that of molecular analogues suggests that little, if any strain is present, which is consistent with the hydrogen being present in the (2×1):H structure (Figs 1(a), 5(a)). The apparent dominance of the monohydride over dihydride-derived infrared features is consistent with the monohydride being the more stable species, as predicted by MM3. We hope to improve the signal-to-noise ratio by modifying the sample holder so as to allow adsorption on both front and back faces and by growing an ultraflat CVD diamond film on the IRE [5]. We plan to determine the thermal stability of the monohydride CH mode and will try to identify conditions under which CH_2 species can be formed.

ACKNOWLEDGMENTS

The authors gratefully acknowledge the National Science Foundation (Grant CHE-8807546) and the Office of Naval Research for support of this work.

REFERENCES

1. (a) J. C. Angus and C. C. Hayman, Science **241**, 913 (1988); (b) W. A. Yarbrough and R. Messier, Science **247**, 688 (1990); (c) F. G. Celii and J. E. Butler, Annu. Rev. Phys. Chem. **42**, 643 (1991).
2. V. B. Aleskovskii and V. E. Drozd, Acta Polytechnica Scandinavica **195** (Proceedings of the 1st International Conference on Atomic Layer Epitaxy), 155 (1990).
3. J. Nishizawa, K. Aoki, S. Suzuki, K. Kikuchi, J. Electrochem Soc. **137**, 1898 (1990), and J. Cryst. Growth **99**, 502 (1990).
4. D. Lubben, R. Tsu, T. R. Bramblett, and J. E. Greene, J. Vac. Sci. Technol. A **9**, 3003 (1991).
5. L. F. Sutcu, M. S. Thompson, C. J. Chu, R. H. Hauge, J. L. Margrave, and M. P. D'Evelyn, Appl. Phys. Lett. **60**, 1685 (1992), (b) L. F. Sutcu, C. J. Chu, M. S. Thompson, R. H. Hauge, J. L. Margrave, and M. P. D'Evelyn, J. Appl. Phys. **71**, 5930 (1992).
6. P. G. Lurie and J. M. Wilson, Surf. Sci. **65**, 453 (1977).
7. T. E. Derry, C. C. P. Madiba, and J. F. P. Sellschop, Nucl. Instrum. Methods **218**, 559 (1983).
8. A. V. Hamza, G. D. Kubiak, and R. H. Stulen, Surf. Sci. **237**, 35 (1990).
9. (a) R. E. Thomas, R. A. Rudder, and R. J. Markunas, in *Diamond Materials*, ed. A. J. Purdes, J. C. Angus, R. F. Davis, B. M. Meyerson, K. E. Spear, and M. Yoder (The Electrochemical Society, Pennington, New Jersey, 1991), p.186; (b) R. E. Thomas, R. A. Rudder, R. J. Markunas, D. Huang, and M. Frenklach, J. Chemical Vapor Deposition (in press).
10. H. K. Schmidt, J. A. Schultz, and Z. Zheng, in *Diamond and Diamond-Like Films and Coatings*, edited by R. E. Clausing *et al.* (Plenum, New York, 1991), p. 669.
11. For example, M. L. Wise, B.G. Koehler, P. Gupta, P.A. Coon, and S.M. George, Surf. Sci. **258**, 166 (1991).
12. W. S. Yang, J. Sokolov, F. Jona, and P. M. Marcus, Solid State Commun. **41**, 191 (1982).
13. (a) B. B. Pate, M. H. Hecht, C. Binns, I. Lindau, and W. E. Spicer, J. Vac. Sci. Technol. **21**, 364 (1982); (b) B. Pate, Surf. Sci. **165**, 83 (1986).
14. B. J. Waclawski, D. T. Pierce, N. Swanson, and R. J. Celotta, J. Vac. Sci. Technol. **21**, 368 (1982).
15. A. V. Hamza, G. D. Kubiak, and R. H. Stulen, Surf Sci. **206**, L833 (1988).
16. (a) T. Sakurai and H. D. Hagstrum, Phys. Rev. B **14**, 1593 (1976); (b) Y. J. Chabal and K. Raghavachari, Phys. Rev. Lett. **54**, 1055 (1985); (c) J. J. Boland, Phys. Rev. Lett. **65**, 3325

(1990); (d) K. Oura, J. Yamane, K. Umezawa, M. Naitoh, F. Shoji, and T. Hanawa, Phys. Rev. B **41**, 1200 (1990); (e) C. C. Cheng and J. T. Yates. Jr., Phys. Rev. B **43**, 4041 (1991); (f) J. E. Northrup, Phys. Rev. B **44**, 1419 (1991); (g) J. J. Boland, Surf. Sci. **261**, 17 (1992); (h) Z. H. Lu, K. Griffiths, P. R. Norton, and T. K. Sham, Phys. Rev. Lett. **68**, 1343 (1992).

17. (a) Y. L. Yang and M. P. D'Evelyn, J. Am. Chem. Soc. **114**, 2796 (1992) and J. Vac. Sci. Technol. A **10**, 978 (1992).
18. D. Huang and M. Frenklach, J. Phys. Chem. **96**, 1868 (1992).
19. "Ultrahigh vacuum apparatus for combined surface science and *in situ* studies of chemical vapor deposition," M. P. D'Evelyn, L. M. Ulvick, L. F Sutcu, Y. L. Yang, S. M. Cohen, E. Rouchouze, and T. Jin, in preparation.
20. Y. L. Yang, Ph.D. Dissertation, Department of Chemistry, Rice University, 1992 (unpublished).
21. S. M. Ko and L. D. Schmidt, Surf. Sci. **42**, 508 (1974).
22. This finding is in agreement with Kubiak and co-workers, who later concluded that the higher-coverage TPD results reported in Ref. 8 were spurious, due to desorption from the Ta support [G. D. Kubiak, presentation at the Fourth Chemical Congress of North America, New York City (August 25-30, 1991)].
23. P. W. Tamm and L. D. Schmidt, J. Chem. Phys. **54**, 4775 (1971).
24. J. B. Marsh and H. E. Farnsworth, Surf. Sci. **1**, 3 (1964).
25. G. Vidali and D. R. Frankl, Phys. Rev. B**27**, 2480 (1983).
26. Y. Mitsuda, T. Yamada, T. J. Chuang, H. Seki, R. P. Chin, J. Y. Huang, and Y. R. Shen, Surf. Sci. **257**, L633 (1991).
27. (a) N. J. Harrick, Phys. Rev. Lett. **4**, 224 (1960); (b) N. J. Harrick, *Internal Reflection Spectroscopy*, (Wiley, New York, 1967); (c) Y. J. Chabal, Surf. Sci. **168**, 594 (1986), and references therein; (d) J. R. Swanson, C. M. Friend, and Y. J. Chabal, J. Chem. Phys. **87**, 6725 (1987); . (e) U. Jansson and K. J. Uram, J. Chem. Phys. **91**, 7978 (1989); (f) J. E. Crowell and G. Lu, Mater. Res. Symp. Proc. **198**, 533 (1990).
28. M. P. D'Evelyn, Y. L. Yang, S. M. Cohen, and L. M. Ulvick, "Ultrahigh vacuum apparatus for infrared multiple-internal-reflection spectroscopy studies on semiconductor surfaces," in preparation.
29. (a) N. L. Allinger, Y. H. Yuh, and J. Lii, J. Am. Chem. Soc.**111**, 8551 (1989); (b) J. Lii and N. L. Allinger, J. Am. Chem. Soc. **111**, 8566 (1989); (c) *ibid* , **111**, 8576 (1989); (d) N.

L. Allinger, F. Li, and L. Yan, J. Comp. Chem. **11**, 849 (1990); (e) N. L. Allinger, F. Li, L. Yan, and J. C. Tai, J. Comp. Chem. **11**, 868 (1990).

30. *MM3(89) Operation Manual*, from Quantum Chemistry Program Exchange, University of Indiana, Bloomington, IN 47405. 1989.
31. Although MM2, the predecessor to MM3, has been applied rather successfully to alkyl radicals [M. R. Imam and N. L. Allinger, J. Molec. Struct. **126**, 345 (1985)], MM3 has not yet been specifically parameterized for radicals [N. L. Allinger, private communication to MPD].
32. P. A. Redhead, Vacuum **12**, 203 (1962).
33. M. P. D'Evelyn, Y. L. Yang, and L. F. Sutcu, J. Chem. Phys. **96**, 852 (1992).
34. M. T. Schulberg, G. D. Kubiak, and R. H. Stulen, Mater. Res. Soc. Symp. Proc. (in press).
35. (a) S. M. Gates, R. R. Kunz, and C. M. Greenlief, Surf. Sci. **207**, 364 (1989); (b) K. Sinniah, M.G. Sherman, L.B. Lewis, W.H. Weinberg, J.T. Yates, Jr., and K.C. Janda, J. Chem. Phys. **92**, 5700 (1990).
36. "Near-first-order desorption kinetics of hydrogen from Ge(100)," M. P. D'Evelyn, S. M. Cohen, E. Rouchouze, Y. L. Yang, and L. F. Sutcu, to be published.
37. R. T. Bailey, Spectrochim. Acta **27A**, 1447 (1971).
38. J. K. Wilmshurst and H. J. Bernstein, Can. J. Chem. **35**, 969 (1957).
39. R. P. Chin, J. Y. Huang, Y. R. Shen, T. J. Chuang, H. Seki, and M. Buck, Phys. Rev. B **45**, 1522 (1992).

(a)

(b)

(c)

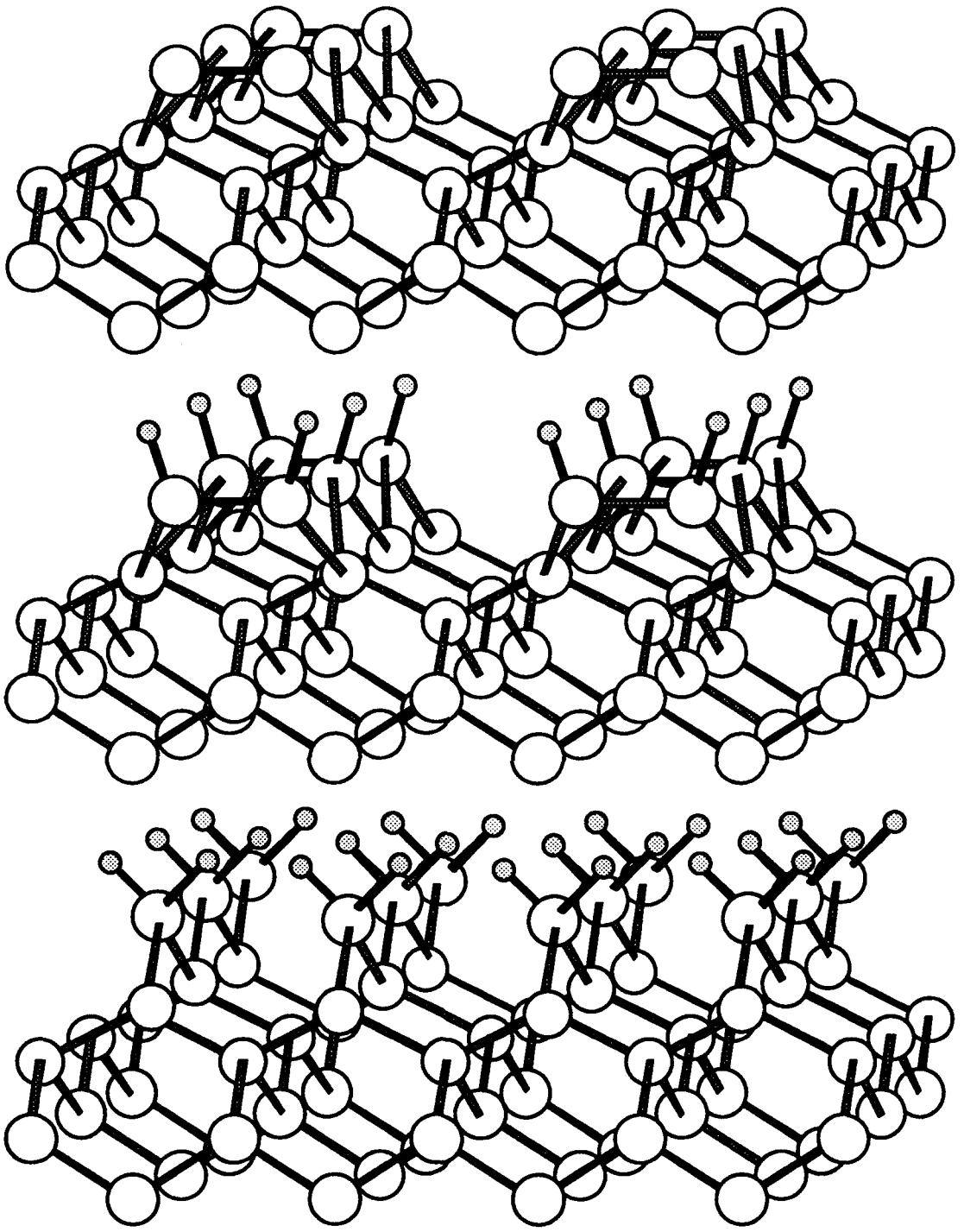

Fig. 1. Schematic illustration of (a) clean diamond (100)-(2×1); (b) the (100)-(2×1):H monohydride, with one hydrogen atom per surface carbon atom; and (c) the (100)-(1×1):2H full dihydride, with two hydrogen atoms per surface carbon atom.

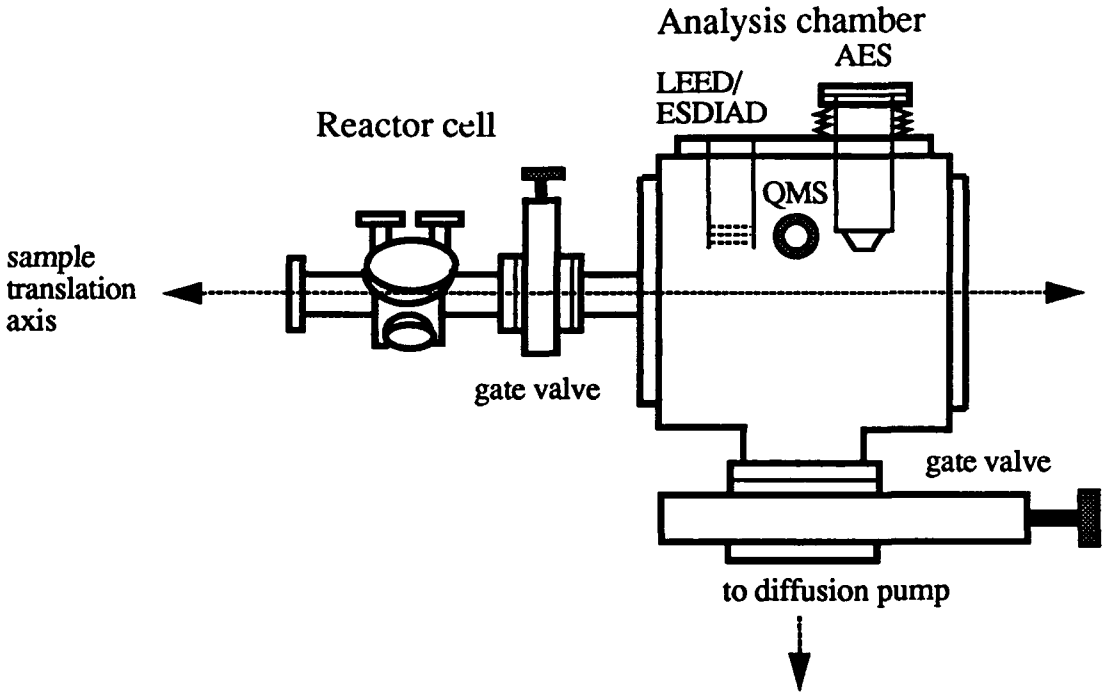
Analysis chamber
AES
LEED/
ESDIAD
Reactor cell
QMS
sample
translation
axis
gate valve
gate valve
to diffusion pump

(a)

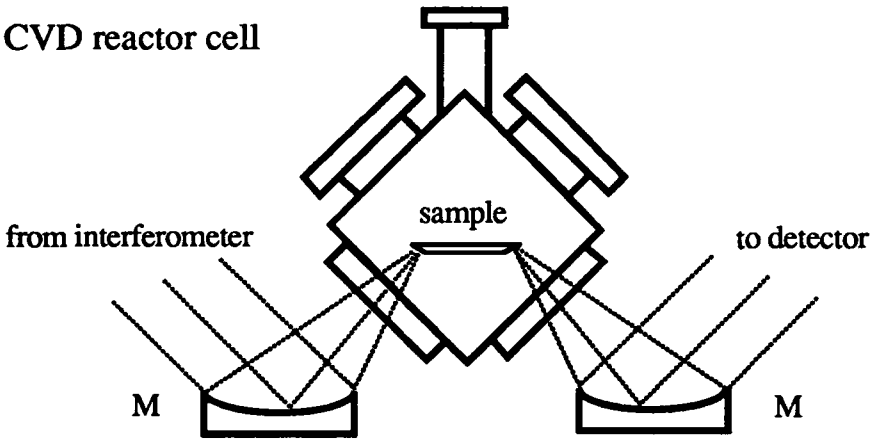
CVD reactor cell
sample
from interferometer
to detector
M
M

(b)

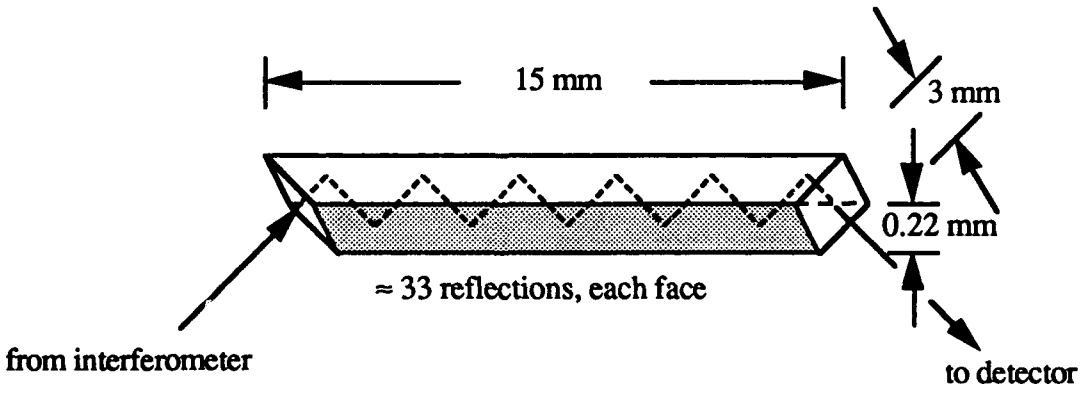
15 mm
3 mm
0.22 mm
≈ 33 reflections, each face
from interferometer
to detector

(c)

Fig. 2. Schematic diagram of combination CVD reactor and UHV analysis apparatus.

(a) Side view of apparatus, with analysis chamber separated from the reactor cell by a gate valve. LEED/ESDIAD: optics for low energy electron diffraction and electron-stimulated desorption ion angular distribution. QMS: quadrupole mass spectrometer. AES: cylindrical mirror analyzer for Auger electron spectroscopy.

(b) End view of reactor cell, showing scheme for infrared multiple-internal-reflection spectroscopy. Collimated light from a FTIR spectrometer is focused from below onto a beveled edge of the diamond (100) crystal sample (S) in the reactor by an *f*/1 off-axis paraboloidal mirror (M), and the transmitted light is collected and focused onto a remote, liquid-nitrogen-cooled narrow-band HgCdTe detector.

(c) Schematic view from below of type IIa natural diamond (100) internal reflection element, $15 \times 3 \times 0.22$ cm^3 in dimension. The IRE has a (100) orientation on the large-area faces, and the end faces are beveled at 45°, providing ≈33 internal reflections from each long face.

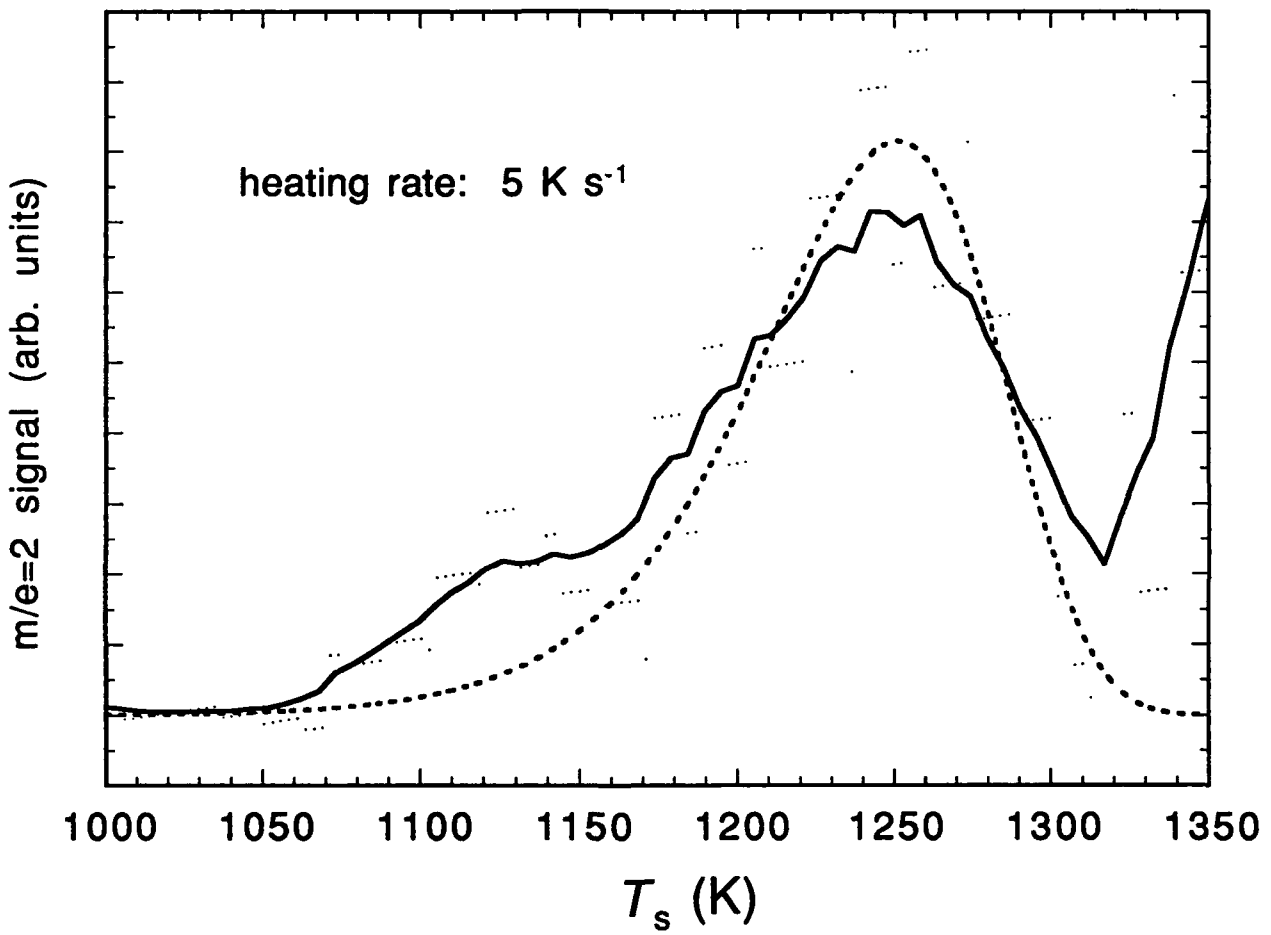

Fig. 3. Temperature-programmed desorption spectrum of H_2 from diamond (100), prepared with a 720 L nominal dose at a sample temperature of 325 K. Solid curve: smoothed raw data (points). The rising signal at temperatures above 1320 K is due to desorption from supports. Dashed curve: calculated desorption trace assuming first-order desorption, a preexponential factor of 10^{13} sec^{-1}, and an activation energy of 79.5 kcal/mol. The heating rate was 5 K s^{-1}.

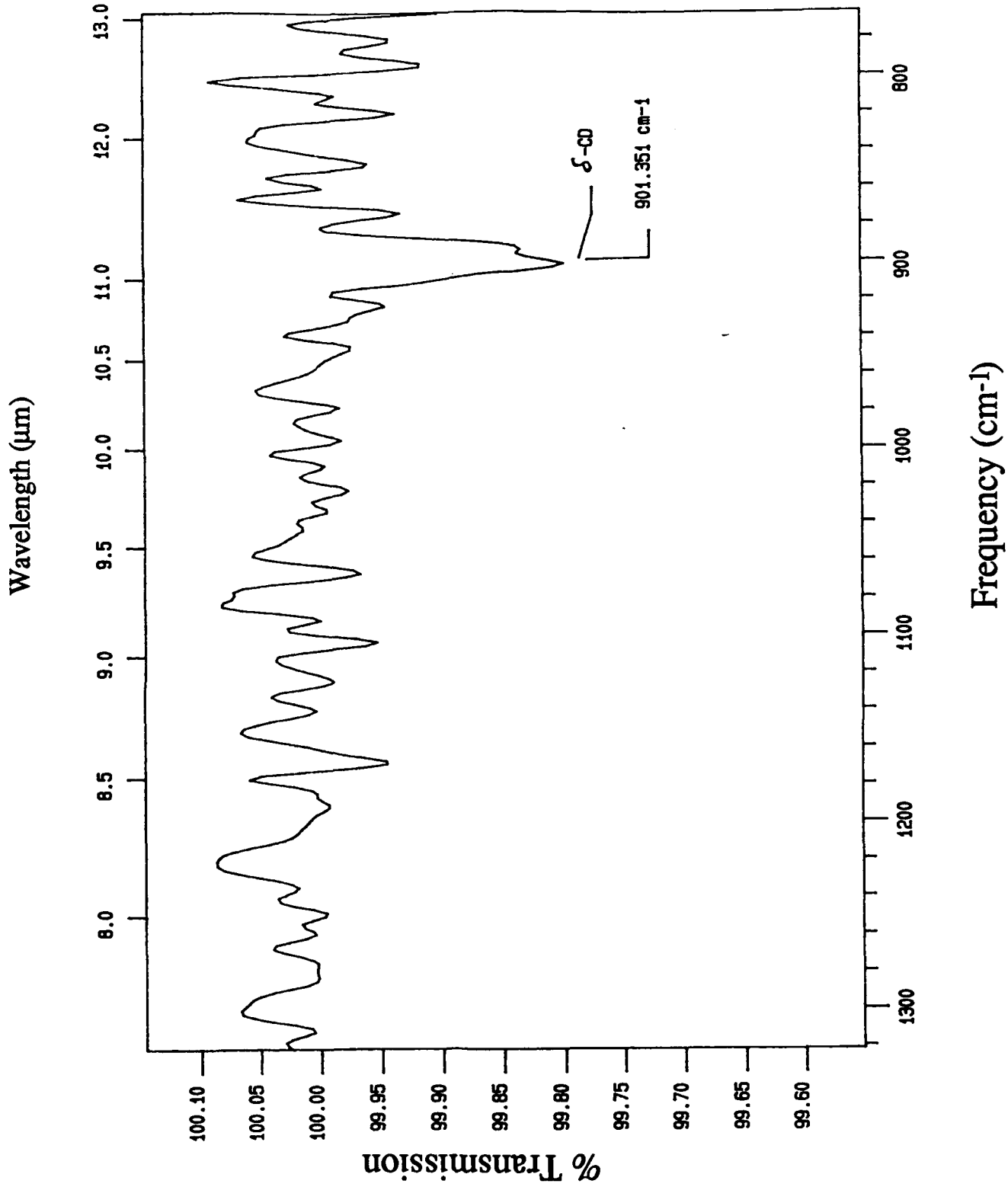

Fig. 4. Infrared multiple-internal reflection spectrum, taken at 4 cm^{-1} resolution with 1024 scans, of CD species on diamond (100). Deuterated surface was prepared with a 7200 L nominal dose at a sample temperature of 500 K.

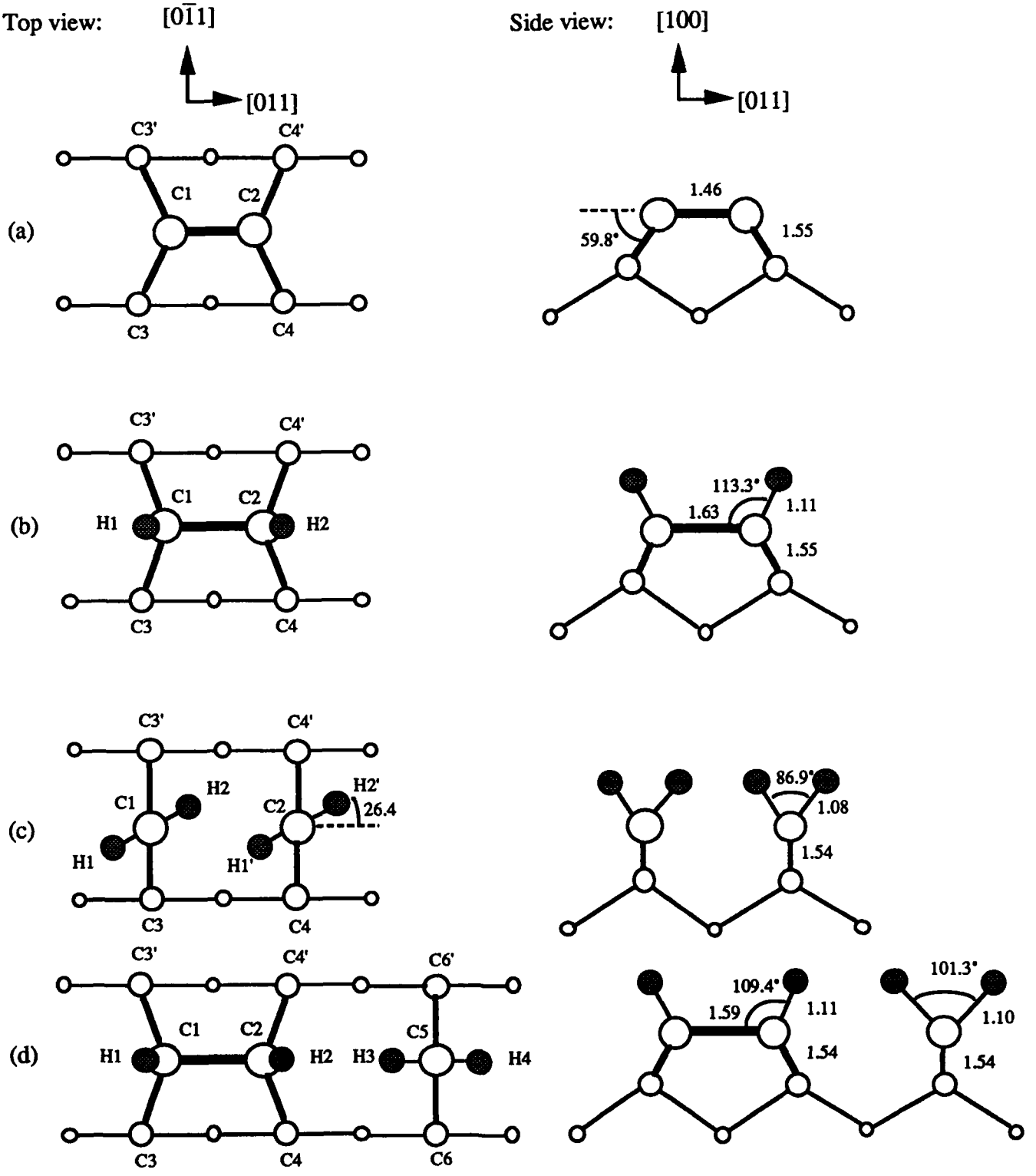

Fig. 5. Top and side views of atomic structures of clean and hydrogenated diamond (100) surfaces: (a) (2×1); (b) (2×1):H; (c) (1×1):2H; and (d) (3×1):1.33H. Bond lengths: Å. ○, ○, and ○: carbon atoms in top, second, and third layers, respectively. ●: hydrogen atoms.